Feshbach-Kerman-Koonin model analysis of preequilibrium (p, p') and (p, n) reactions at 12 to 26 MeV

Y. Watanabe, A. Aoto, and H. Kashimoto
Department of Energy Conversion Engineering, Kyushu University, Kasuga, Fukuoka 816, Japan

S. Chiba, T. Fukahori, K. Hasegawa, M. Mizumoto, S. Meigo, M. Sugimoto, and Y. Yamanouti
Japan Atomic Energy Research Institute, Tokai, Ibaraki 319-11, Japan

N. Koori
Faculty of Integrated Arts and Sciences, The University of Tokushima, Tokushima 770, Japan

M. B. Chadwick
Nuclear Data Group, Lawrence Livermore National Laboratory, Livermore, California 94551

P. E. Hodgson
Nuclear Physics Laboratory, Physics Department, University of Oxford, Oxford OX1 3RH, United Kingdom
(Received 22 September 1994)

Double-differential proton emission cross sections have been measured for proton-induced reactions on ^{98}Mo and ^{106}Pd at incident energies around 26 MeV. Several sets of (p, p') and (p, n) data for both target nuclei at incident energies from 12 to 26 MeV are analyzed in terms of the multistep-direct (MSD) and multistep-compound (MSC) reaction models of Feshbach, Kerman, and Koonin (FKK). The strength V_0 of the effective N-N interaction is extracted from a fit of the calculated MSD spectrum to the experimental data using the subtraction method of isolating and analyzing the MSD component alone. A similar analysis is also applied to (p, p') and (n, n') data for ^{93}Nb in the same energy region. The experimental nucleon emission spectra at 26 MeV are reproduced well by the calculation that includes preequilibrium MSD and MSC emission, direct collective excitation to low-lying discrete levels, and Hauser-Feshbach equilibrium emission in a quantum-mechanical way. The systematic dependence of V_0 on the incident energy and the nature of projectiles and ejectiles is investigated. In addition, the sensitivities to input parameters used in the MSD calculation (the optical model potential parameters, the pairing correction, and the nonlocality correction) are examined in order to see their effect on the determination of V_0. The possibility of gradual absorption of reaction flux from the P to the Q chain is also discussed through analyses of preequilibrium (p, p') and (p, n) spectra using a phenomenological phase space approach.

PACS number(s): 25.40.−h, 24.60.Dr, 24.60.Gv, 24.50.+g

I. INTRODUCTION

The quantum-mechanical theory of Feshbach, Kerman, and Koonin (FKK) [1] has been successfully applied to preequilibrium nucleon emission from nucleon-induced reactions over a wide range of incident energies [2,3]. Increasing interest is now directed to more precise analyses which allow us to improve the models and approximations used in the FKK theory. Through such analyses, it is of great interest to establish a reliable set of model parameters involving the strength V_0 of the effective N-N interaction which is treated as the only free parameter. This is important not only for the basic study of nuclear reaction mechanisms but also for the application to nuclear data evaluation. The main purpose of this work is to investigate the systematics of the strength V_0 and the sensitivity to input parameters in nucleon-induced reactions at low incident energies.

We focus primarily on proton-induced reactions at incident energies below 30 MeV. Most of the FKK analyses in this energy region have so far been carried out for (n, n') and (p, n) reactions [2,3]. Proton data are usually more suitable for precision analyses than neutron data because of the good statistics. Proton data, therefore, enable us to study more details of the reaction mechanism, such as the incident energy dependence and the isotope effect of target nuclei (e.g., shell and odd-even effects). Since there are many (p, n) data which were measured systematically at incident energies around 26 MeV by the Hamburg group [4–7], we have measured proton emission spectra for the same target and incident energies in order to make a simultaneous analysis of (p, p') and (p, n) data. There are also the experimental (p, p') spectra for ^{98}Mo and ^{106}Pd at 12, 14, 16, and 18 MeV from the Kyushu group [8,9]. Hence these two isotopes were chosen for our new experiment at incident energies around 26 MeV in order to investigate the incident energy dependence of the statistical multistep reaction.

As for neutron-induced reactions, Chadwick and Young [10] have recently applied their FKK-GNASH code system to the reactions on ^{93}Nb at 14, 20, and 25.7

MeV and analyzed the whole emission spectra of neutrons and protons and angular distributions in a unified quantum-mechanical way. As a result, they found that the multistep-direct (MSD) mechanism dominates preequilibrium emission even for incident energies as low as 14 MeV and multistep-compound (MSC) emission is less important than many previous analyses suggested. In addition, they have pointed out that MSD-MSC crossover ($P \rightarrow Q$) transitions play an essential role in giving a satisfactory description of preequilibrium reactions under the requirement of reaction flux conservation. Although such crossover transitions have been discussed by other authors [2,3,11,12], all the discussions were based mainly on analyses of neutron data with rather poorer statistics than proton data. Thus it is worthwhile to extend such analyses to a variety of proton-induced reactions at low incident energies.

The FKK-GNASH code [10] is used in the present analyses of both (p,p') and (p,n) data for ^{98}Mo and ^{106}Pd in order to examine its applicability to proton-induced reactions at low incident energies. Our particular interest is to know the systematic trend of the only free parameter V_0. In the FKK formalism used in the FKK-GNASH code, the MSD component depends only on the parameter V_0. Therefore we need to separate the MSD component from experimental inclusive emission spectra. For this purpose, we apply the subtraction method [13] to isolate the MSD component by taking forward-backward differences in the center-of-mass system, and study the dependence of the extracted strength V_0 on the incident energy and the reaction channel. Also, the (n,n') and (p,p') reactions on the same target ^{93}Nb are analyzed to investigate the Coulomb and isospin effects in the preequilibrium nucleon emission. Furthermore, we study the sensitivity of MSD cross sections to some input parameters (i.e., the optical potential parameters, the pairing correction, and the nonlocality correction) in order to see how they affect the determination of the effective strength V_0.

In the FKK-GNASH code, $P \rightarrow Q$ transitions at the initial $2p1h$ stage are taken into account by a reduction factor R_{MSC} defined as the ratio of bound to total phase space, and all other $P \rightarrow Q$ fluxes generated at more complex stages are assumed to decay eventually from equilibrium stage without MSC emission. Namely, the MSC emission following $P \rightarrow Q$ transitions at complex preequilibrium stages beyond the $2p1h$ stage is neglected in the code. On the other hand, Marcinkowski *et al.* [12] have recently proposed an extended FKK formalism of MSC emission, so that $P \rightarrow Q$ transitions at more complex preequilibrium stages, i.e., so-called gradual absorption in preequilibrium stages, can be included through a reduction factor calculated by the ratio of bound to total phase space at each stage. Such an MSD-MSC crossover has more recently been justified theoretically by Arbanas *et al.* [14] on the basis of a linked MSD-MSC multistep reaction model which is more rigorous than the phenomenological phase space approach. In this work, therefore, we take into account the gradual reaction flux absorption using the phase space model [12] for simplicity, and study the effect of $P \rightarrow Q$ transitions and the subsequent MSC emission in proton-induced reactions at low incident energies.

Our (p,p') experiment is described together with the experimental results in Sec. II. The formulation of the FKK model is outlined in Sec. III. Results of FKK analyses using the subtraction method and comparisons with experimental data are presented in Secs. IV A to IV D. The extracted strength V_0 of the effective N-N interaction is summarized with regard to the incident energy dependence in Sec. IV E. The sensitivity of the MSD cross section to input parameters is described in Sec. V A. Some systematic behavior found in the extracted V_0 is discussed in Sec. V B. The gradual absorption effect in preequilibrium (p,p') and (p,n) reactions is investigated in Sec. V C. Finally, the conclusions of this work are summarized in Sec. VI.

II. EXPERIMENT AND RESULTS

A. Experimental procedure and data processing

The experiment was performed using a proton beam from the JAERI tandem accelerator; its energy was 25.6 MeV for ^{98}Mo and 26.0 MeV for ^{106}Pd, respectively. The proton beam was transported to a scattering chamber 50 cm diameter and focused on a target within a beam size of about 2 mm diameter. During the measurement, the beam intensity was monitored by means of a current integrator connected to a Faraday cup and the beam current was adjusted in a range from about several tens of nA to about 300 nA in accordance with the detector angle. Targets of ^{98}Mo and ^{106}Pd were self-supporting metallic foils. The thicknesses and isotopic enrichment were 0.45 mg/cm^2 and 97.1% for ^{98}Mo and 1.02 mg/cm^2 and 98.48% for ^{106}Pd.

A ΔE-E counter telescope consisting of two silicon surface-barrier detectors which are 300 and 5000 μm thick, respectively, was used to detect all emitted charged particles separately and suppress background events due to γ rays. A defining aperture 3.0 mm in diameter made of stainless steel was placed just in front of the ΔE detector and located 147 mm from the target. Signals from each detector were processed using electronic circuits assembled with commercially available standard NIM modules. A particle identification (PI) module was employed to separate signals corresponding to each emitted particle (protons, deuterons, tritons, and alphas). Finally, two output signals from the module, $\Delta E + E$ and PI, were stored as two-dimensional data using a PC-based multiparameter data acquisition system. Note that the above-mentioned experimental setup and procedure has been reported in detail elsewhere [15].

Energy spectra of emitted protons were measured at angles in intervals of 10° from 30° to 150°. However, the data measured at 30° are excluded in the following data analysis, since the spectrum was found to contain obviously continuous background, or a large tail of an elastic peak due to edge scattering by the defining aperture, and the background was not perfectly subtracted. With regard to elastic scattering cross sections, additional measurements were made at smaller angles of 20°, 25°, and

30°, in order to determine the absolute cross sections by normalizing the experimental elastic cross sections to the optical model prediction at such small angles. The absolute uncertainty involved in the normalization was estimated to be less than 8%. The double-differential cross sections were converted to the c.m. system and the angle-integrated data for the continuum portion of the measured proton spectra were obtained by a Legendre polynomial fitting of experimental angular distributions for each energy bin of 0.2 MeV.

B. Experimental results

Experimental double-differential proton emission spectra are shown at 40°, 90°, and 140° for ^{98}Mo and ^{106}Pd by solid circles in Figs. 1 and 2, as some typical samples. All error bars indicated are only statistical ones. One may notice that there are no experimental data at outgoing proton energies below about 7 MeV. The reason why protons with such energies were not measured is because they were stopped completely in the ΔE detector. As can be seen in these figures, the continuum region lying between 10 and 20 MeV exhibits smooth and forward-peaked angular distributions characterizing preequilibrium particle emission. In the following FKK analysis, it will become clear that the MSD process is dominant in preequilibrium proton emission.

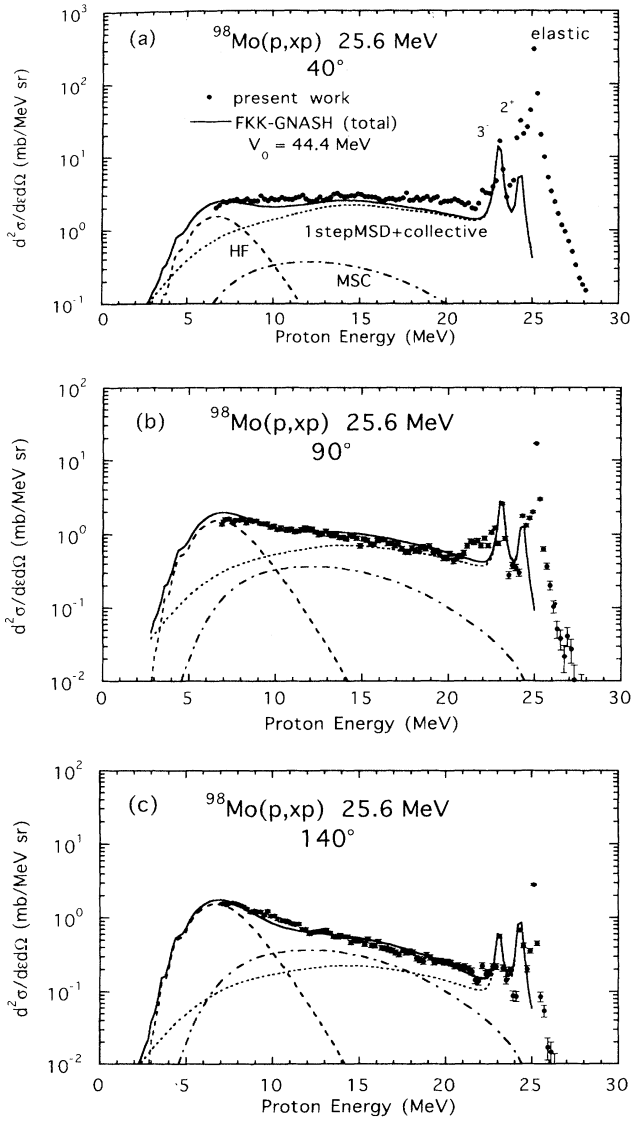

FIG. 1. Experimental double-differential cross sections for the ^{98}Mo(p, xp) reactions at 25.6 MeV (solid circles) and those calculated with the FKK-GNASH code. See text for details of the calculation.

III. FKK MODEL FORMULA

Here we summarize the formulas of the FKK model used in the present analysis. The detailed description is given in Ref. [10].

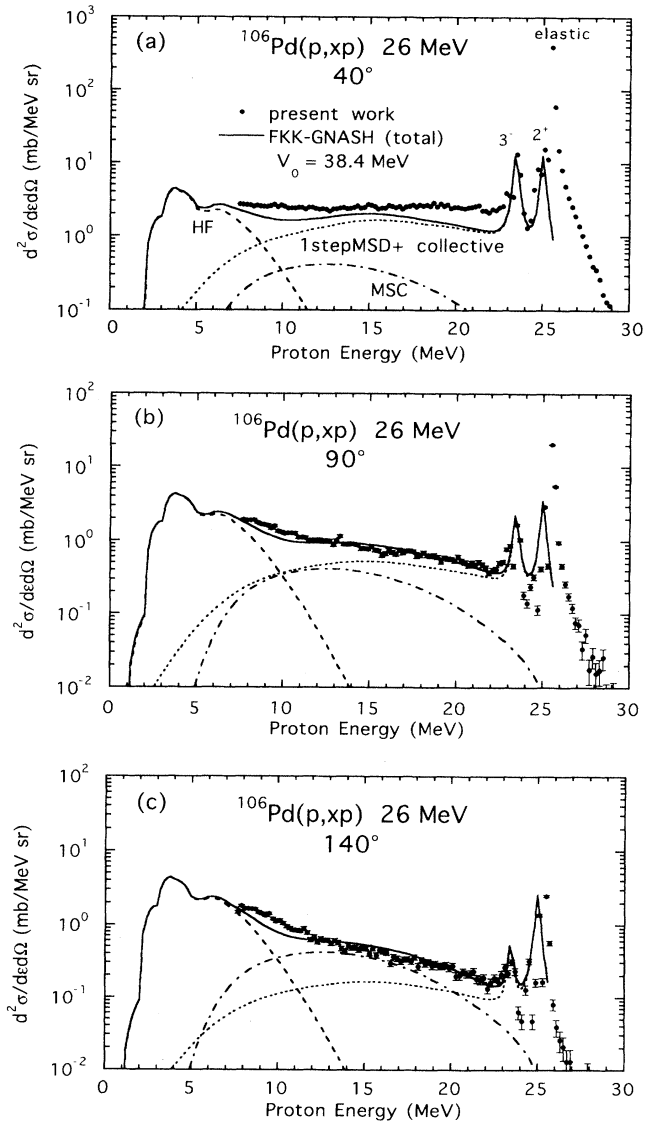

FIG. 2. Same as Fig. 1, but for the ^{106}Pd(p, xp) reactions at 26 MeV.

A. Multistep direct reactions

In our analysis, we consider only one-step scattering in MSD processes because two-step scattering is negligibly small for incident energies below 30 MeV, as we will describe later in Sec. IV A. It is also unnecessary to take into account multiple preequilibrium emission [16] for reactions at such low incident energies. Accordingly, we describe only the one-step MSD expression below.

The one-step double-differential cross section for transition from an initial state (E_0, Ω_0) to final continuum states with $[E, E+dE]$ and $[\Omega, \Omega+d\Omega]$ is given by the following simple expression:

$$\left.\frac{d^2\sigma(E,\Omega \leftarrow E_0\Omega_0)}{d\Omega\, dE}\right|_{1\text{ step}} = \sum_l (2l+1)\rho(1p,1h,E_0-E,l) \times \left\langle \left[\frac{d^2\sigma(E,\Omega \leftarrow E_0\Omega_0)}{d\Omega}\right]_l^{\text{DWBA}} \right\rangle, \quad (1)$$

where l is the transferred orbital angular momentum. The quantity $\rho(1p,1h,E_0-E,l)$ is the density of $1p$-$1h$ states with excitation energy $U = E_0 - E$ and is given by a product of the Williams expression taking into account the finite well depth [17]:

$$\omega(p,h,U) = \frac{g^n}{p!h!(n-1)!}\sum_{j=0}^{h}(-1)^j \binom{h}{j} \times (U-\Delta-A_{ph}-j\varepsilon_F)^{n-1} \times \Theta(U-\Delta-A_{ph}-j\varepsilon_F) \quad (2)$$

with $p = h = 1$ and $n = p + h$ and the spin distribution function

$$R_n(l) = \frac{2l+1}{2\sqrt{2\pi}\sigma_n^3}\exp\left[-\frac{(l+\frac{1}{2})^2}{2\sigma_n^2}\right] \quad (3)$$

with the spin cutoff parameter σ_n. The quantities Δ, A_{ph}, and ε_F in Eq. (2) are the pairing energy correction, the Pauli principle correction factor $A_{ph} = (p^2 + h^2 + p - 3h)/4g$, and the Fermi energy. The Θ function is unity if its argument is positive, and zero otherwise.

$\langle [d\sigma(E,\Omega \leftarrow E_0,\Omega_0)/d\Omega]_l^{\text{DWBA}} \rangle$ is the average of distorted-wave Born approximation (DWBA) cross sections exciting $1p$-$1h$ states of energy $U = E_0 - E$ which are determined by a spherical Nilsson model. The DWBA cross sections are calculated microscopically using a Yukawa potential of range 1 fm and strength V_0 for $1p$-$1h$ excitations.

B. Multistep compound reactions

Following Chadwick and Young [10], we use the transmission coefficient calculated from a conventional optical model to determine the reaction flux into the MSC chain. The differential MSC cross section is given by

$$\frac{d\sigma}{dE} = \pi\lambda^2 \sum_J (2J+1)[R^{\text{MSC}}T_J] \sum_{N=1}^{r}\sum_{\nu l}\frac{\langle\Gamma_{nJ}^{\uparrow\nu l}(U)\rangle}{\langle\Gamma_{nJ}\rangle} \times \left(\prod_{M=1}^{N-1}\frac{\langle\Gamma_{MJ}^{\downarrow}\rangle}{\langle\Gamma_{MJ}\rangle}\right), \quad (4)$$

where $R^{\text{MSC}}T_J$ is the transmission coefficient for forming bound $2p$-$1h$ states of spin J multiplied by a reduction factor R^{MSC}. This factor can be estimated as the ratio of bound to total $2p$-$1h$ phase space, and calculated with the restricted and unrestricted Williams expressions. The running index N represents the preequilibrium class and n is the number of excitons with $n = p + h = 2N + 1$. The first two preequilibrium stages ($N = 1$ and 2) are considered as MSC emission occurring before the equilibrium "r stage" as in Ref. [10]. J and l are the composite system spin and orbital angular momenta of the emitted particle, respectively. $\Gamma^{\uparrow}$, $\Gamma^{\downarrow}$, and Γ denote the emission width, the damping width, and their sum (the total width), respectively. These quantities are calculated microscopically with a zero-range potential $V(\mathbf{r}_1,\mathbf{r}_2) = V_0(\frac{4}{3}\pi\mathbf{r}_0^3)\delta(\mathbf{r}_1-\mathbf{r}_2)$, and are finally expressed as a product of X functions and Y functions. The detailed description of X and Y functions is given in Ref. [10]. It should be noted that the FKK assumption of constant wave functions is made in the calculation of the bound-continuum and bound-bound overlapping integrals included in the X functions. As a result, the MSC emission spectrum is independent of V_0 by the cancellation in the ratio of emission to total widths. Hence the MSC calculation has no free parameter if the reduction factor R^{MSC} is estimated from the ratio of bound and total phase spaces of $2p$-$1h$ doorway states. As in Ref. [10], the double-differential MSC cross sections are calculated by dividing Eq. (4) by 4π.

IV. ANALYSIS AND RESULTS

A. Calculational details and input parameters

We have analyzed the nucleon-induced reactions listed in Table I, using the FKK-GNASH code [10]. The principal input parameters used in the MSD and MSC calculations are summarized in Table II. The Walter-Guss optical potential [21] is used for both neutrons and protons. This option is different from that used in Ref. [10]. The reason will be discussed in Sec. V A 1, together with a test of the sensitivity of the MSD cross section to optical potential parameters. The single-particle level density $g = A/13$, where A is the nuclear mass number, and the spin cutoff parameter of Gruppelaar [22] are the same as in Ref. [10]. No pairing energy correction [i.e., $\Delta = 0$ MeV in Eq. (2)] is used because of the experimental observation that there is no appreciable pairing effect on preequilibrium spectra, as will be shown in detail in Sec. V A 2. In addition, we introduce the correction due to the nonlocality of the distorting potentials in terms of the so-called Perey factor [23]. The nonlocality range is taken to be 0.85 fm [23]. The effect of the nonlocal-

TABLE I. The nucleon-induced reactions analyzed in this work.

Reaction	Target	Incident energy	Reference
(p,p')	^{98}Mo	12, 14, 16, 18, and 25.6 MeV[a]	Watanabe *et al.*[b,c]
(p,p')	^{106}Pd	12, 14, 16, 18, and 26 MeV[a]	Watanabe *et al.*[b,c]
(p,p')	^{93}Nb	18 MeV	Watanabe *et al.*[b]
(p,n)	^{98}Mo	25.6 MeV	Mordhorst *et al.*[d]
(p,n)	^{106}Pd	26 MeV	Hölbling *et al.*[e]
(n,n')	^{93}Nb	14.1, 18, 20, 25.7 MeV	Takahashi *et al.*[f]
			Matsuyama *et al.*[g]
			Marcinkowski *et al.*[h,i]

[a]The present experiment for 25.6 and 26 MeV (p,p').
[b]Reference [8].
[c]Reference [9].
[d]Reference [6].
[e]Reference [7].
[f]Reference [18] for 14.1 MeV.
[g]Reference [19] for 18 MeV.
[h]Reference [12] for 20 MeV.
[i]Reference [20] for 25.7 MeV.

ity on the MSD cross section will be discussed later in Sec. V A 3.

In the MSD calculation with a set of input parameters shown in Table II, the strength V_0 of the effective N-N interaction is the only adjustable parameter. The V_0 value is determined for each reaction, so that the calculated MSD spectrum fits the experimental one obtained using the subtraction method [13]. This extracts the MSD contribution by taking the forward and backward difference of the cross sections at complementary c.m. angle pairs (e.g., 30°-150°), since the MSC contribution as well as that due to the equilibrium decay give angular distributions symmetric about 90° in the c.m. system. In the preliminary MSD calculation, we have estimated the two-step MSD contribution for 25.6 MeV (p,p') on ^{98}Mo, and confirmed that its contribution is as negligibly small (at most 5%) in the preequilibrium region as for (n,n') in Ref. [10]. We can say, therefore, that the one-step MSD process alone is a good approximation at incident energies below 26 MeV only if normal DWBA matrix elements are used to describe intermediate transitions in multistep-direct processes. Although it has been reported [14] that the multistep contribution increases when we use non-normal DWBA matrix elements, the one-step MSD emission is still dominant at the incident energy considered here.

Direct collective excitations of low-lying states are observed as several distinct peaks in the high emission energy region of (p,p') spectra as shown in Figs. 1 and 2. Since the direct collective excitation cannot be described within the framework of the FKK model, it should be included using the usual DWBA calculation with a collective form factor. In this work, we include only the first 2^+ and 3^- states as low-lying vibrational levels using the DWUCK4 code [24]. The excitation energies and deformation parameters are taken from nuclear tables [25,26]. For an odd nucleus ^{93}Nb, the weak coupling model is adopted and the excitation energies and deformation parameters for ^{92}Zr are used. Finally, direct collective cross sections calculated for the first 2^+ and 3^- states are smeared using a Lorentzian function with a full width at half maximum (FWHM) corresponding to the experimental resolution.

After calculating the MSD and MSC emission cross sections ($\sigma_{\rm MSD}$ and $\sigma_{\rm MSC}$) with the FKK model and the direct collective cross section ($\sigma_{\rm col}$) with the DWUCK4 code [24], we use the Hauser-Feshbach code GNASH [27] to describe not only equilibrium particle decay from the primary compound nucleus but also the sequential decay of residual nuclei. Unitarity, or reaction flux conservation, is satisfied in our calculation, so that the total reaction cross section is equal to the sum of the direct and preequilibrium cross sections ($\sigma_{\rm MSD} + \sigma_{\rm MSC} + \sigma_{\rm col}$) and the primary equilibrium cross section. The input parameters for the GNASH code calculation are the stan-

TABLE II. The principal input parameters used in the MSD and MSC calculations.

(1) Optical potential	Walter-Guss[a]
(2) Single-particle level density parameter	$g = A/13$
(3) Spin cutoff parameter	$\sigma^2 = 0.24nA^{2/3}$ [b]
(4) Pairing energy correction	None ($\Delta = 0$ MeV)
(5) Nonlocality range	$\beta = 0.85$ fm[c]

[a]Reference [21].
[b]Reference [22].
[c]Reference [23].

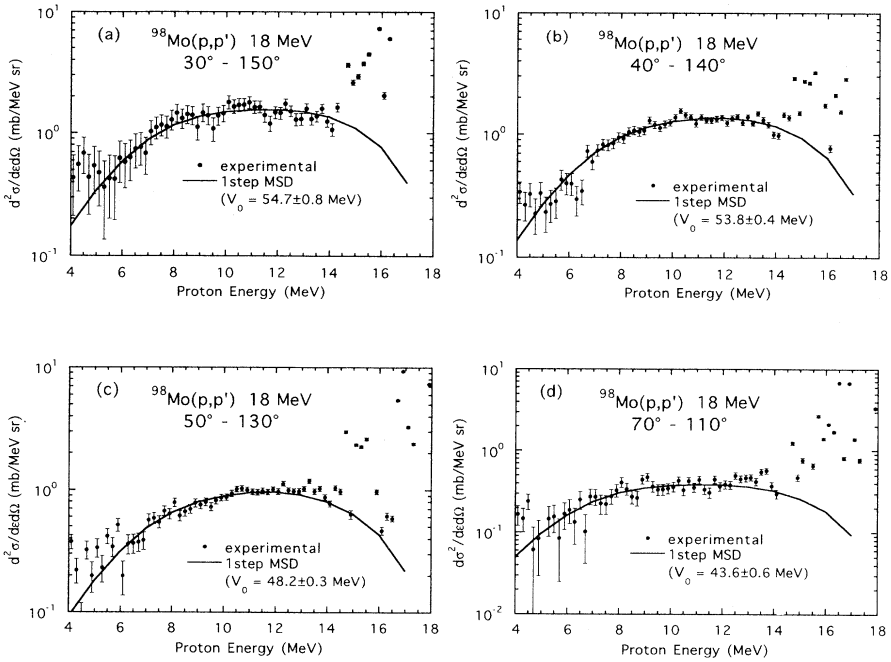

FIG. 3. Subtracted double-differential cross sections for 18 MeV (p, xp) on ^{98}Mo for four pairs of complementary angles. The solid curves are subtracted double-differential cross sections of the one-step MSD component calculated with the FKK-GNASH code [10]. The curves are normalized to the data and the extracted best fit V_0 and the error are indicated in each figure. The experimental data are taken from Ref. [8].

dard ones: the same optical potential parameters as in the FKK calculation and the level density parameters of Gilbert and Cameron [28].

In the following subsections, we present the results of the subtraction method and compare the FKK-GNASH calculations with the experimental double-differential nucleon emission spectra and the angle-integrated energy spectra for the reactions listed in Table I.

B. (p, p') reactions on ^{93}Nb, ^{98}Mo, and ^{106}Pd

Typical results of the subtraction method are shown for ^{98}Mo(p, p') reactions at 18 and 25.6 MeV in Figs. 3 and 4. In each case, the theoretical MSD cross section (only one step) was normalized to the data by adjusting the strength V_0. The best fit V_0 value was determined

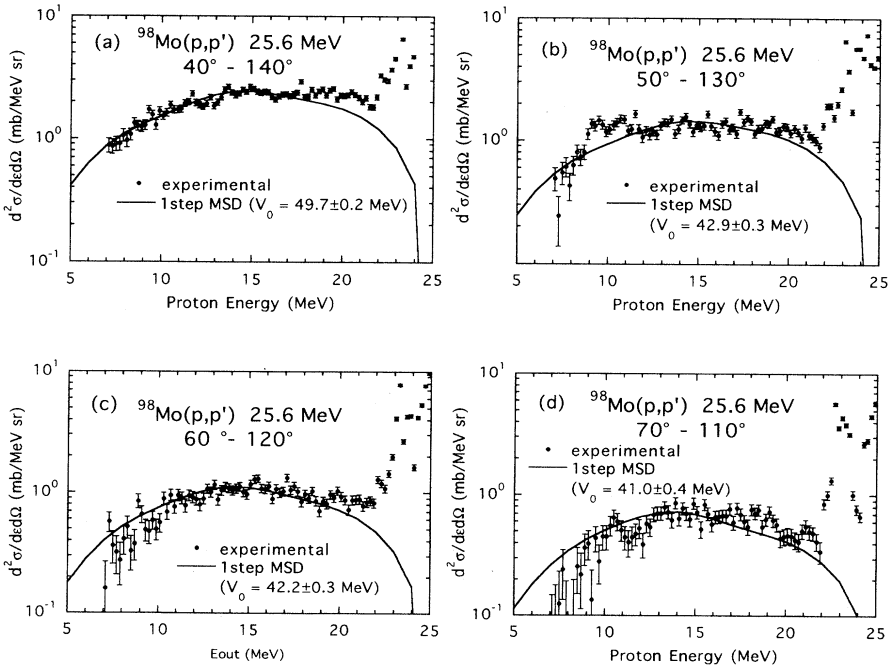

FIG. 4. Same as Fig. 3, but for the ^{98}Mo(p, xp) reactions at 25.6 MeV.

using the least-squares method and the final average V_0 value ($\bar{V}_0$) for each reaction was obtained by taking the following weighted average:

$$\bar{V}_0 = \sqrt{\overline{V_0^2}} = \sqrt{\frac{\sum_i V_0^2(\theta_i) \sin\theta_i \omega_i}{\sum_i \sin\theta_i \omega_i}}, \quad (5)$$

where $V_0(\theta_i)$ is the best fit V_0 value at a given complementary angle pair $(\theta_i, \pi - \theta_i)$ and ω_i is the statistical weight.

The MSD calculation fits the data very well at intermediate emission energies but not at higher emission energies where there is a large contribution from the direct excitation of low-lying collective states. Similarly, good fits were obtained for the other (p,p') reactions listed n Table I. These results show that the subtraction method is a quite useful method of extracting the strength V_0 from the experimental data.

Figures 1 and 2 show the calculated double-differential proton emission spectra for ^{98}Mo at 25.6 MeV and ^{106}Pd at 26 MeV compared with the experimental ones. The dotted lines give the sum of the MSD component calculated with the average strengths V_0 given in the figures and the calculated direct collective excitation to the first 2^+ and 3^- states. The MSC components calculated using Eq. (4) are shown by the dash-dotted lines. The total proton emission spectra (the solid lines) are obtained by adding the Hauser-Feshbach (HF) equilibrium spectra (the dashed lines). The calculation is in overall good agreement with the experimental emission spectra over a wide emission energy and angular region. It can also be seen that the component of direct process decreases gradually with increasing angle but is still a large fraction even at the backward angle of 140°. This indicates that the MSD process is important in (p,p') at low incident energies.

In Figs. 1 and 2, we find some underprediction in the higher-energy region at a forward angle of 40°, which may be related to the existence of collective excitation with higher multipolarities except the first 2^+ and 3^- and/or the contamination of the continuous background due to edge scattering. In addition, the calculated (p,p') spectra show a dip at outgoing energies around 10 MeV. Since the subtracted MSD spectra give a good description of the experimental ones in the energy region as shown in Fig. 3, the disagreement seems to be due to the MSC and/or equilibrium emission calculation. This issue will be discussed from the viewpoint of $P \rightarrow Q$ transitions of reaction flux, through analyses of the angle-integrated (p,p') spectra in Sec. V C.

Although there is some disagreement as mentioned above, it is worthwhile to emphasize that this successful result was obtained by combination of the MSD calculation based on the subtraction method and the MSC calculation with no free parameter using the FKK-GNASH code. This implies that the calculational method used in this work is equivalent to that used for (n,n') of Ref. [10] and $P \rightarrow Q$ transitions considered through the reduction factor R^{MSC} play an essential role in the (p,p') as well.

C. (p,n) reactions on ^{98}Mo and ^{106}Pd

The data for the ^{98}Mo(p,n) reaction at 25.6 MeV [6] and ^{106}Pd(p,n) reaction at 26 MeV [7] were also analyzed using the FKK-GNASH code. Some results of the subtraction method for ^{98}Mo(p,n) are shown in Fig. 5. The calculated one-step MSD spectra show excellent agreement with experiment except at the low-energy end. The best fit V_0 value is indicated in each figure. Those values are not so scattered among each pair as in the (p,p') case where the best fit V_0 value tends to increase as the

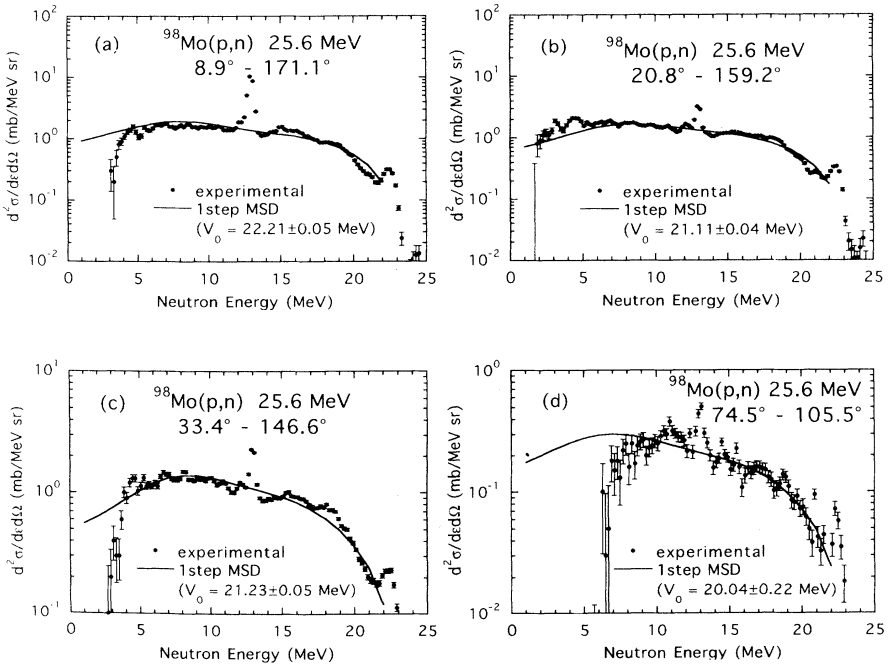

FIG. 5. Same as Fig. 3, but for the ^{98}Mo(p,xn) reactions at 25.6 MeV. The experimental data are taken from Ref. [6].

forward angle becomes small. The obtained average V_0 values are 21.5 ± 0.3 MeV for ^{98}Mo and 20.3 ± 0.7 MeV for ^{106}Pd, respectively.

The double-differential neutron emission spectra calculated with the average V_0 values are compared with the experimental ones in Figs. 6 and 7. The dotted and the dash-dotted curves are the one-step MSD component and the MSC component, respectively. Their sum is shown by the solid curve. The calculation reproduces quite well the high-energy continuum portion of the experimental spectrum, although there is some overestimation around the peak of an isobaric analog state (IAS) and some underestimation in the neutron energy region between 4 and 8 MeV. Similar behavior as in (p,p') is seen with respect to variation in the ratio of MSD to MSC components with angle. The one-step MSD process is found to be important for neutron emission even at large angles.

The extracted V_0 values are about one-half those for the (p,p') reaction on the same target and incident energy. Namely, the MSD analysis for the proton-induced reaction for the same incident energy and target nucleus requires a large difference in V_0 between neutron emission and proton emission. Other simultaneous analyses of (p,p') and (p,n) reactions on ^{90}Zr for higher incident energies of 80 and 160 MeV [16] also show similar systematics on the extracted V_0. The difference in V_0 between (p,p') and (p,n) will be discussed again in Sec. V B.

D. ^{93}Nb(n,n') reactions

We have analyzed ^{93}Nb(n,n') data for incident energies of 14.1 MeV [18], 18 MeV [19], 20 MeV [12], and 25.7 MeV [20] to extract the strength V_0 for (n,n') at

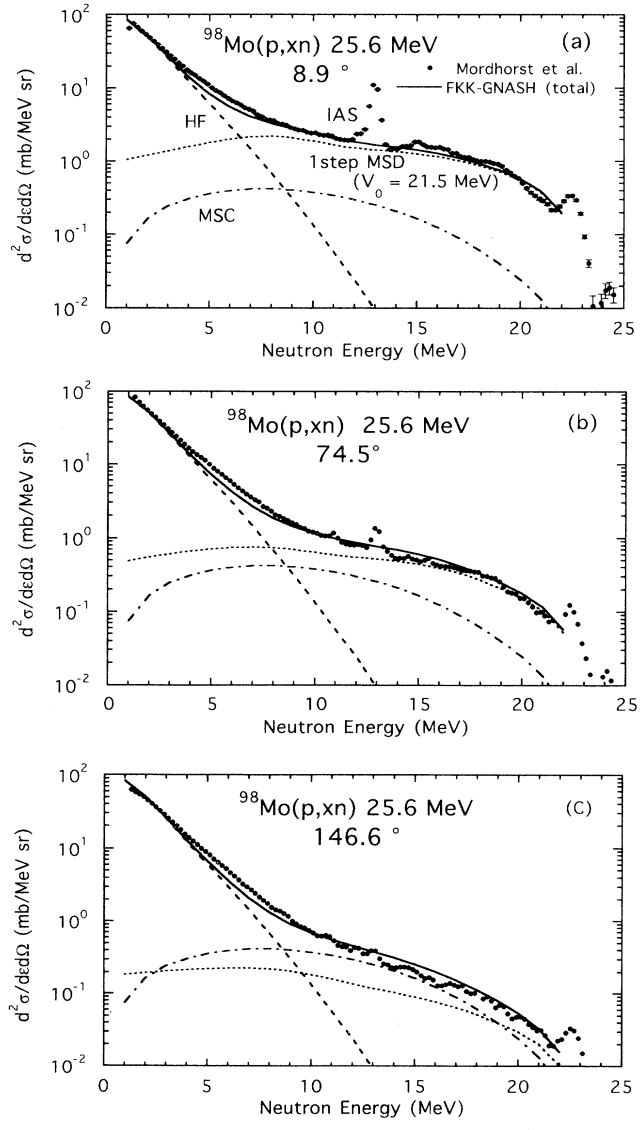

FIG. 6. Comparison of the calculated double-differential cross sections of the ^{98}Mo(p,xn) at 25.6 MeV with the experimental ones taken from Ref. [6].

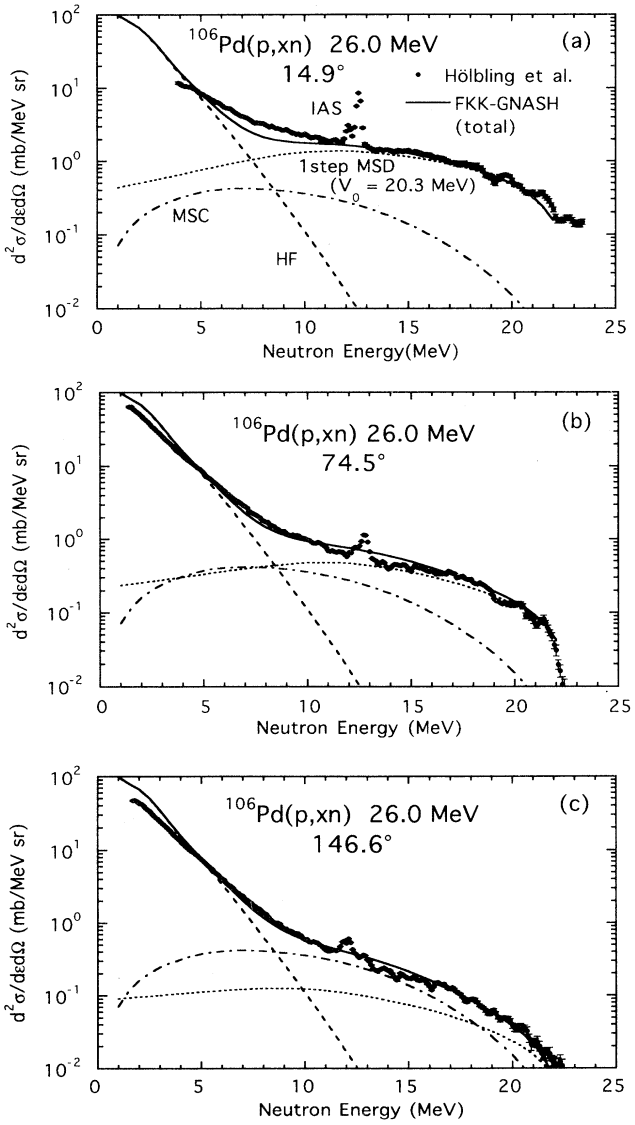

FIG. 7. Same as Fig. 6, but for the ^{106}Pd(p,xn) reaction at 26 MeV. The experimental data are taken from Ref. [7].

low incident energies with the default input parameter listed in Table II. In this work, the subtraction method was applied only to the data at 14.1 MeV because there are few appropriate pairs of double-differential cross section (DDX) data measured at complementary angles for the other energies. In the subtraction analysis, the calculated one-step MSD spectra gave good agreement with the experimental ones at neutron emission energies below 10 MeV, as in Ref. [13]. The extracted V_0 value is 42.8 ± 2.1 MeV. Note that this value is rather larger than those obtained in Refs. [10,13], because different input parameters and corrections were used; i.e., the optical potential parameters, the pairing energy correction, and the nonlocality correction. For the data at the other incident energies, the V_0 value for the one-step MSD process is determined by equating MSD emission with the difference between the data and MSC emission in the same way as used in Ref. [10].

A typical calculated angle-integrated (n, n') spectrum for 14.1 MeV is compared with the experimental one in Fig. 8. The one-step direct component including collective excitation and the MSC component are shown by the dotted and the dash-dotted lines, respectively. The dashed line is the HF component including both $(n, 2n)$ and (n, pn) emission. The calculated total spectrum shows excellent agreement with the experimental data in the intermediate outgoing energy region between 4 and 10 MeV where the preequilibrium neutron emission is predominant. The HF calculation overpredicts the data in the region below 4 MeV, but a similar trend is also seen in the calculation [10] with the same input parameters as in this work except for the optical potential parameters. Note that no input parameters for the HF calculation have been adjusted so as to get the best fit to the data in this region. The underestimation seen in the collective excitation region over 10 MeV may be partly due to a large tail of an elastic peak around 14 MeV.

E. The strength V_0 of effective N-N interaction

In Fig. 9, we plot the strength V_0 of the effective N-N interaction extracted from our analyses as a function of incident energy. Table III also gives the numerical values. The V_0 values for (p, p') for ^{98}Mo and ^{106}Pd increase monotonically with decreasing incident energy, whereas the values for (n, n') are nearly constant within the errors. The V_0 values for (p, p') satisfy an approximate relation $V_0 = \text{const}/\sqrt{E_{\text{inc}}}$ shown by the solid line. We also estimated the energy variation of V_0 by assuming that it has the same energy dependence as the real part of the nuclear optical potential [2] and normalizing to the extracted V_0s at 26 MeV using the Walter-Guss potential [21]. The result is given by the dotted line $V_0 = 48.3 - 0.31 E_{\text{inc}}$. The energy dependence is found to be rather weak and similar to the V_0s for (n, n'), but not for (p, p'). As for the (p, n) reactions, the V_0 value is different from that of (p, p') by a factor of about 2 for the same energy and same target, as has been mentioned in Sec. IV C. Our possible interpretation of such systematic behavior of V_0 will be described in Sec. V B.

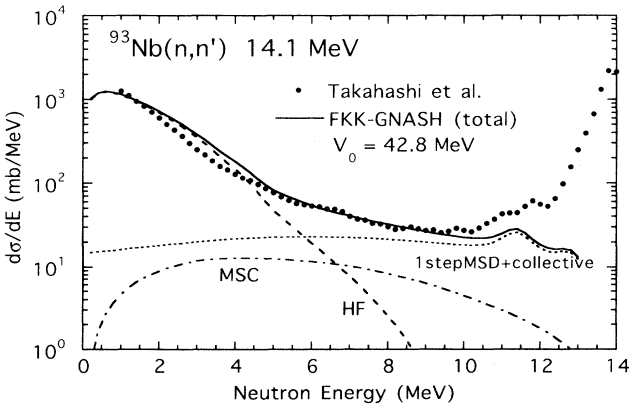

FIG. 8. The calculated angle-integrated spectra for ^{93}Nb(n, xn) at 14.1 MeV and the experimental data. The experimental data are taken from Ref. [18].

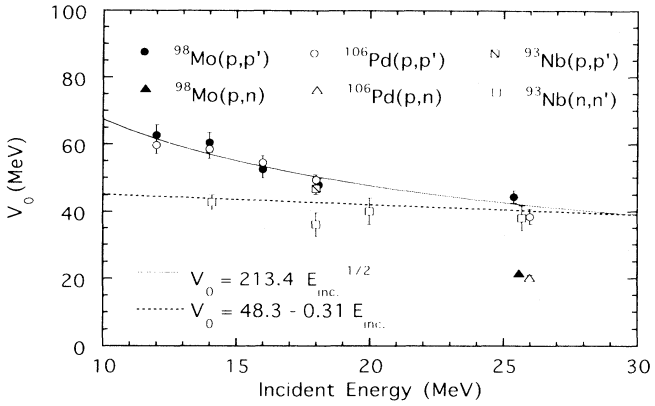

FIG. 9. The extracted strength V_0 plotted as a function of the incident energy.

TABLE III. Numerical table of the extracted V_0 values.

Reaction	Incident energy (MeV)	V_0 (MeV)
^{98}Mo (p, p')	12	62.7 ± 3.1
	14	60.5 ± 3.0
	16	52.5 ± 2.6
	18	47.9 ± 1.9
	25.6	44.4 ± 1.8
^{98}Mo (p, n)	25.6	21.5 ± 0.3
^{106}Pd(p, p')	12	59.7 ± 2.6
	14	58.5 ± 2.8
	16	54.5 ± 2.0
	18	49.4 ± 1.5
	26	38.4 ± 2.4
^{106}Pd(p, n)	26	20.3 ± 0.7
^{93}Nb(n, n')	14.1	42.8 ± 2.1
	18	36.0 ± 3.6[a]
	20	40.0 ± 4.0[a]
	25.7	38.0 ± 3.7[a]
^{93}Nb(p, p')	18	46.8 ± 1.7

[a]The subtraction method was not applied. See details in text.

V. DISCUSSIONS

A. Sensitivity of the MSD cross section to input parameters

1. Opticle model potential (OMP) parameter

In our analysis, the Walter-Guss (W-G) potential [21] was used for both neutrons and protons as global optical potentials for incoming and outgoing distorted waves. The Wilmore-Hodgson (W-H) potential [29] for neutrons and the Becchetti-Greenlees (B-G) potential [30] for protons were used in the previous calculations with the FKK-GNASH code [10]. Besides them, several global nucleon optical potentials are known for low energies below 30 MeV. It is of interest to see how the choice of OMP parameters affects the effective interaction strength V_0. Such an investigation was made for an MSD analysis of (p,p') for higher incident energies of 100 to 200 MeV by Richter *et al.* [31], who have shown the importance of the choice of OMP parameters in the extraction of V_0 values.

A similar investigation has been carried out for nucleon inelastic scattering at lower incident energies, i.e., ^{98}Mo(p,p') at 18 MeV and ^{93}Nb(n,n') at 14.1 MeV. The result is shown in Fig. 10. The following global parameter sets are used. B-G [30], Perey [32], Menet *et al.* [33], and W-G [21] potentials for protons, and W-H [29], B-G [30], Rapaport, Kulkarni, and Finlay [34], and W-G [21] potentials for neutrons. It should be noted that the same V_0 value extracted with the W-G potential is employed in all calculations. Figure 10 shows that there is obviously a strong dependence on the OMP parameters used, especially with respect to the magnitude, although the shape of the energy spectra is quite similar except for the (n,n') spectrum calculated with the potential of Rapaport, Kulkarni and Finlay [34]. As a result, it was found that the extracted V_0 value depends strongly upon the choice of the OMP parameter set for low incident energies. Accordingly, one should pay attention to which optical potential was applied when one compares the V_0 values reported by different authors.

In our FKK analyses for incident energies below 30 MeV, we decided to choose the W-G potential parameters. There are two main reasons for the choice. First, it is better to use the same OMP potential over the whole energy range to avoid an undesirable discontinuity that may be introduced by using different global parameter sets according to the energy region. Second, it is more reasonable to use neutron and proton OMP potentials in which the asymmetry term has the same magnitude but different sign for neutrons and protons, in order to see the effect on preequilibrium emission from simultaneous analyses of (p,p') and (p,n) reactions.

Here we show an example of the above-mentioned discontinuity of the MSD cross section at a certain energy. The one-step MSD (n,n') spectrum calculated using the FKK-GNASH code is shown for ^{93}Nb at 21 MeV in Fig. 11. Two different OMP parameters (B-G and W-H) were used in the calculation of incident distorted waves for comparison, but the same W-H parameter for the outgoing distorted waves. The dotted and the solid lines

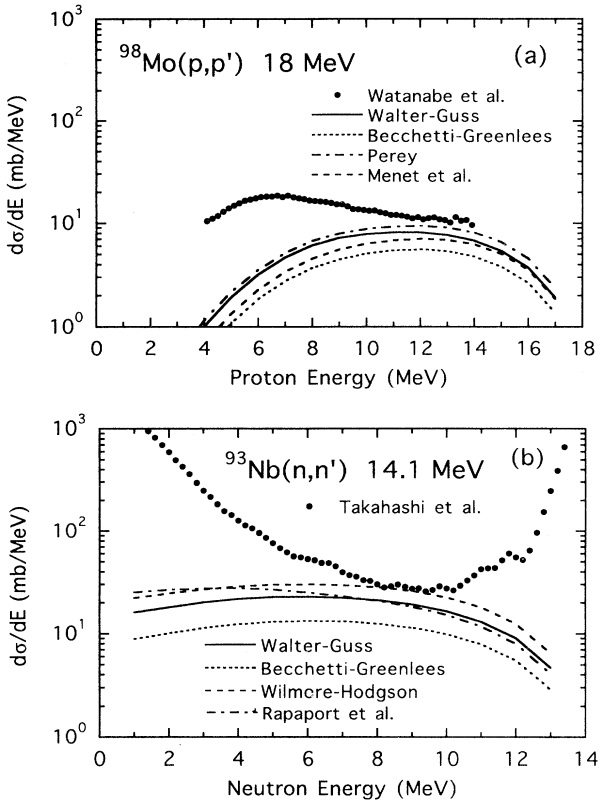

FIG. 10. The sensitivity of the one-step MSD spectrum to optical potential parameters. (a) 18 MeV (p,p') on ^{98}Mo and (b) 14.1 MeV (n,n') on ^{93}Nb.

represent the results with the B-G and the W-H potentials, respectively. Both shapes are quite similar, but the magnitude is obviously different. The latter (W-H) is about 1.5 times larger than the former (B-G). As a result, the difference in V_0 amounts to about 22% to obtain the same absolute one-step MSD cross section. Such a

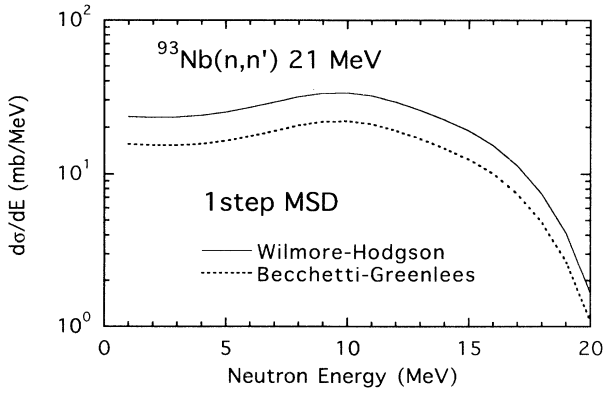

FIG. 11. The calculated one-step MSD cross sections of ^{93}Nb(n,n') at 21 MeV. The Becchetti-Greenlees (B-G: dotted line) [30] and the Wilmore-Hodgson (W-H: solid line) [29] potentials are used for incident channels. The same W-H potential is used for outgoing channels for both cases. As for the strength V_0, the same value is used for both calculations.

discontinuity is undesirable in studies of the dependence of V_0 on incident energy.

2. *Pairing correction*

The pairing correction [Δ in Eq. (2)] in the p-h state density has been taken into account explicitly in many of the previous applications [2,3,10] of the FKK model, whereas no pairing correction is adopted in this work. In this subsection, the validity of omitting the pairing correction is discussed from the viewpoint of the odd-even effect on the preequilibrium spectrum.

First, the sensitivity to the pairing correction is examined for ^{98}Mo(p,p') reactions at 18 and 25.6 MeV using the subtraction method and the results are shown in Fig. 12. The dotted curves are the subtracted (p,p') spectra calculated with the pairing energy of Dilg *et al.* [35] ($\Delta = 2.59$ MeV) and the solid curves are those without pairing correction ($\Delta = 0$ MeV). For both incident energies, the calculation without pairing correction is in much better agreement with the experimental spectra corresponding to the MSD component over the whole continuous region than that with the pairing correction.

Next, a comparison of the experimental data [8] is made between an odd- and even-even neighbor pair of ^{nat}Ag and ^{106}Pd in Fig. 13. The figure shows a comparison between the subtracted spectra (50°-130°). Both

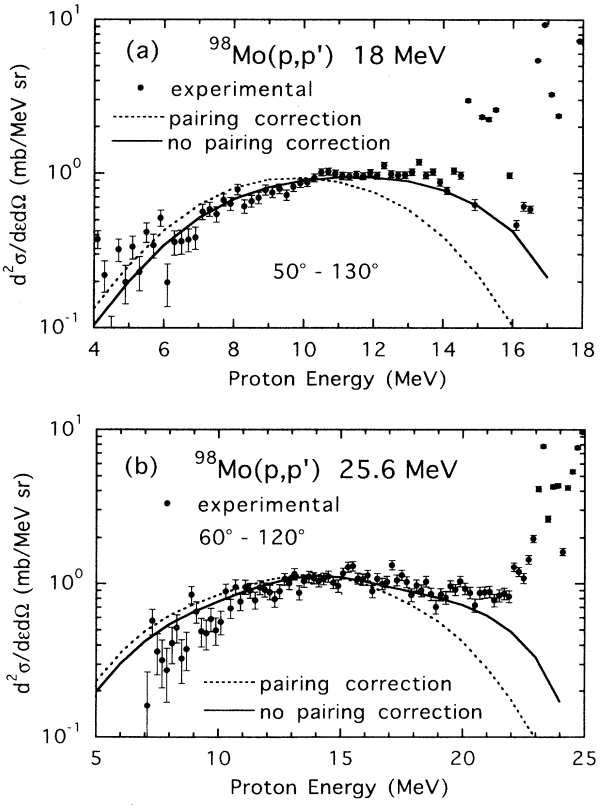

FIG. 12. Comparison of the subtracted ^{98}Mo(p,xp) spectra calculated with and without pairing correction with the experimental data: (a) 18 MeV [8] and (b) 25.6 MeV.

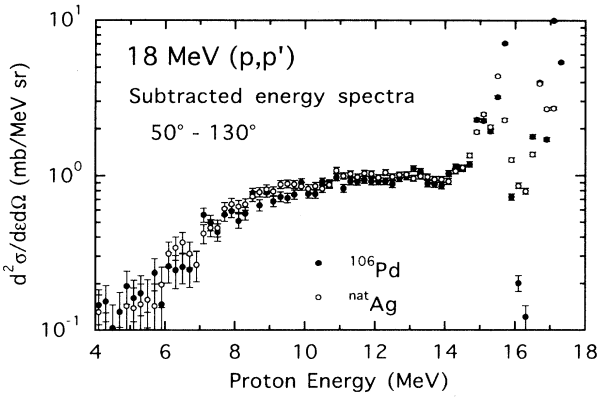

FIG. 13. Experimental data of subtracted double-differential cross sections of ^{106}Pd(p,xp) and Ag(p,xp) scattering for the complementary angle pair of 50°-130°. The experimental data are taken from Ref. [8].

spectra are quite similar over the whole energy region including collective excitation and there is no appreciable odd-even effect in an MSD (p,p') spectrum. This is also true of the other angle pairs. It is thus preferable to use either no pairing correction or the same pairing energy for a neighboring pair of an even-even nucleus and an odd nucleus in order to provide good agreement between the MSD calculation and the experiment. No pairing correction would be preferable with regard to better agreement with the shape of the MSD spectrum, as shown in Fig. 12.

Here we consider the reason why there is no appreciable odd-even effect in an MSD component of (p,p') scattering. The one-step MSD cross section is proportional to the density of $1p$-$1h$ states of the residual nucleus as given by Eq. (1). The other quantities except the partial state density ω_{1p1h} are considered to be independent of the odd-even effect. The DWBA cross sections are calculated with optical model wave functions and shell model wave functions varying smoothly with the mass number, and the spin-dependent term [Eq. (3)] is not affected by the odd-even difference. Accordingly, only the p-h state density given by Eq. (2) contains the odd-even difference as the pairing correction.

The pairing correlation can be considered under the quasiparticle approximation often used in nuclear structure calculations. The $1p$-$1h$ states of the residual nucleus corresponds to the two quasiparticle (q.p.) state. The excitation energy of one q.p. state is

$$E_{\text{q.p.}} = \sqrt{(\varepsilon - \lambda)^2 + \Delta^2}, \tag{6}$$

where ε is the single-particle (s.p.) energy, λ the Fermi energy, and Δ the pairing energy determined by the odd-even mass differences corresponding to the pairing correction energy given by Dilg *et al.* [35].

The s.p. level scheme is transformed into the q.p. level schemes using Eq. (6). In an even-even nucleus, there is no q.p. level between 0 and Δ MeV and the level spacing approaches that of the s.p. level as excitation energy increases. On the other hand, for an odd-even nucleus, there are levels arising from an unpaired nucleon

between 0 and Δ MeV, but the higher excitation states become almost the same as those of the even-even nucleus. Thus the effect of pairing correlation is expected to appear only at very low excitation energies, less than Δ. Watanabe *et al.* [8] have reported the microscopic calculation of partial state densities using the q.p. approximation for ^{106}Pd and ^{107}Ag and found that there is no appreciable odd-even effect on the $1p$-$1h$ state density at excitations higher than the pairing energy 2Δ of the even-even nucleus. If the $(n)(n)^{-1}$ configuration is also considered, the odd-even effect becomes even more negligible at higher excitation energies compared with the case of the $(p)(p)^{-1}$ configuration alone, because both nuclei contain the same number of neutrons. Furthermore, the odd-even effect in single-particle excitation states, such as $1p$-$1h$ states, is likely to be hidden by the strong collective excitation structure observed at low excitation energies below about 2Δ in the case of (p,p') scattering as shown in Figs. 12 and 13.

3. Nonlocality correction

In our analysis, the nonlocality correction with range $\beta = 0.85$ fm [23] was used in the MSD and direct collective calculations. Here we discuss the effect on the calculated cross section. Figure 14 shows a comparison of the one-step MSD energy spectra with the nonlocality correction (the solid line) and without it (the dotted line) for ^{98}Mo(p,p') reactions at (a) 12 and (b) 25.6 MeV. The other input parameters are the same as listed in Table II. The strength V_0 is fixed to that extracted in the analysis mentioned in Sec. IV A. The nonlocality correction is found to reduce the one-step MSD cross section by about 35%, regardless of the incident energy. This reduction is explained by the so-called "Perey effect" which reduces the amplitude of the incoming and outgoing distorted waves inside the nucleus. As can be seen in Fig. 14, the spectral shape is almost independent of the nonlocality correction. As a result, the nonlocality correction leads to larger strength V_0 compared with the strength extracted without the correction. It should be noted that the nonlocality correction has little effect on the shape of angular distributions.

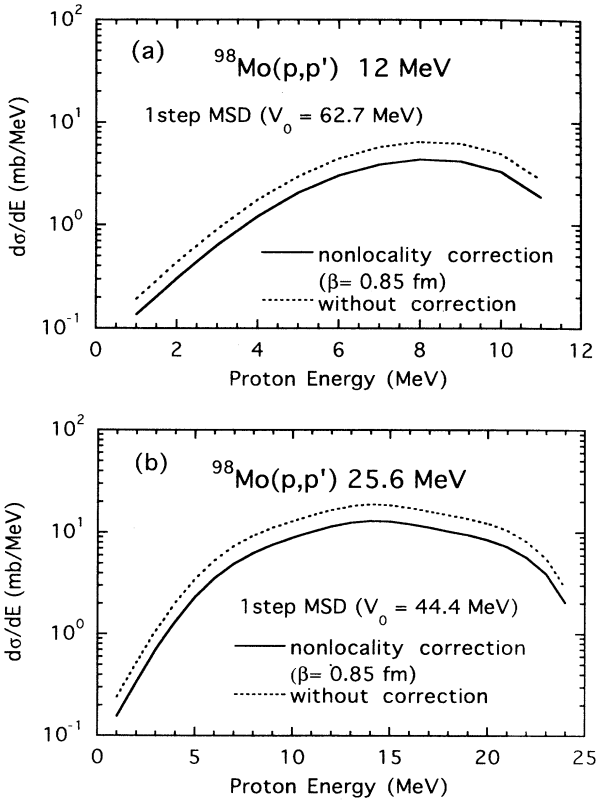

FIG. 14. Sensitivity of the one-step MSD cross sections to the nonlocality correction for the ^{98}Mo(p,p') scattering at (a) 12 and (b) 25.6 MeV.

Recently, an intercomparison between the FKK-GNASH code [10] and the MSD code developed by Bonetti and Chiesa [36] has been made by Watanabe, Avrigeanu, and Richter [37]. The intercomparison revealed that the nonlocality correction had been used in the previous work [2,3] with the latter MSD code. Accordingly, we will need to use the correction when we discuss the sensitivity of the MSD cross sections to the input parameters compared with those previous results. Also, the importance of the correction at low incident energies was shown in the semiclassical distorted-wave model analysis made by Watanabe and Kawai [38]. Therefore the nonlocality correction was incorporated in our FKK analysis of the one-step MSD process including collective excitation.

B. Systematic trends of the strength V_0

Some features of the strength V_0 extracted in this work are summarized as follows (see Fig. 9).

(a) The V_0 values extracted from (p,p') for incident energies from 12 to 26 MeV are nearly proportional to $1/\sqrt{E_{\rm inc}}$, whereas the energy dependence of V_0 for (n,n') is similar to the energy dependence of the real part of the nuclear optical potential within the errors.

(b) There is a difference in V_0 values between (p,p') and (n,n') at the same incident energy.

(c) The V_0 for (p,p') is considerably different from that for (p,n) for the same target nucleus and incident energy.

Our extracted energy dependence of V_0 for (p,p') was also found by the (n,n') analysis [10] and by Koning [39] who used a collective form factor with the deformation parameter β. Here we provide some brief comments on the difference between our systematics and the others. Our result for (n,n') is different from that in Ref. [10] and shows a somewhat weak energy dependence. The extracted V_0 values are also different from the values extracted in the other FKK analyses [2,3] in which the Bonetti-Chiesa code [36] was used and are generally larger than those. The major reason is due to the input parameters and corrections used, as has been discussed in the preceding subsection. Our (p,p') calculation is the first FKK analysis at incident energies below 30 MeV. To establish the V_0 systematics, therefore, the FKK-GNASH

analyses with the standard parameter set listed in Table II will be necessary for a lot of experimental data over a wider range of target mass number and incident energy.

For our finding that the V_0 values from (n,n') analyses are smaller than those from (p,p') at the same incident energy, the following interpretation is given by paying attention to the difference in the charge and isospin of the projectile. The kinetic energy of an incident nucleon inside the target nucleus is equivalent to the local energy $E_c(\mathbf{r})$ by the local energy approximation

$$E_c(\mathbf{r}) + U_{c,\mathrm{eff}}(\mathbf{r}) = E_c, \tag{7}$$

where c denotes neutron or proton, $U_{c,\mathrm{eff}}(\mathbf{r})$ is the effective potential energy [40] calculated with both the real term and the imaginary term, and E_c is the incident energy. Since there is a large Coulomb potential near the surface region where (p,p') scattering is known to occur predominantly at low incident energies, the proton local energy in the vicinity of the surface is largely different from the neutron local energy because of the Coulomb barrier, which is nearly 10 MeV for the targets which we have analyzed. As the incident proton energy decreases, the Coulomb barrier affects the local energy of the incident proton. In addition, the isospin term in the real and imaginary potentials also leads to a difference in the local energies because the sign is opposite for a neutron and for a proton. Therefore the effective energy of an incident nucleon interacting with a target nucleon is different for a neutron and a proton inside the nucleus even if the incident energy outside the nucleus is same.

To test the above-mentioned difference, the V_0 values for ^{98}Mo(p,p') and ^{93}Nb(n,n') are plotted in Fig. 15 against the local energy at the radius $R = 1.25A^{1/3}$ fm, where A is the mass number. These V_0 values show a rather smooth variation with the local energy, compared with Fig. 9. The dotted line is a result fitted with a simple equation $V_0 = \mathrm{const}/E_{\mathrm{local}}$. Hence it seems reasonable to introduce the idea of the local energy in order to interpret the difference in the V_0 values between (p,p') and (n,n') scattering at the same low incident energy. It should be noted, however, that the energy dependence

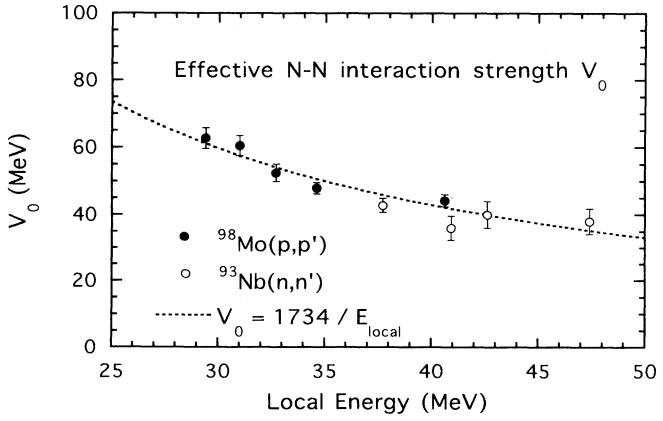

FIG. 15. The extracted values of the strength V_0 as a function of local energy. See the text for details.

of V_0 is not the same as that of the real part of the nuclear optical potential, although the V_0 for both (p,p') and (n,n') is expressed by the smooth function of local energy as shown in Fig. 15. According to this idea of the local energy, the difference in V_0 between (p,p') and (n,n') is expected to become very small as the incident energy increases and becomes much larger than $U_{c,\mathrm{eff}}(\mathbf{r})$. Our discussion is, however, based only on the analysis of a few data for target nuclei with the mass number around 100. Further analyses of much more experimental (p,p') and (n,n') data will be necessary to draw a clear conclusion.

Next, we consider the reason why the extracted V_0 values are obviously different for the (p,p') and (p,n) reactions. In the FKK calculation, we use the one-component MSD formalism in which the neutron and proton distinguishability is not taken into account. If the distinguishability is introduced into the calculation, the p-h states of the residual nucleus excited by the (p,p') scattering are clearly different from those excited by the (p,n) reaction. For the one-step (p,p') scattering, two kinds of configurations consisting of proton-particle and proton-hole $(p)(p)^{-1}$ and neutron-particle and neutron-hole $(n)(n)^{-1}$ are allowed, whereas only the configuration with proton-particle and neutron-hole $(p)(n)^{-1}$ is excited by the one-step (p,n) reaction. As a result, the density of residual $1p$-$1h$ states excited by the (p,n) reaction is about a half that for the (p,p') scattering at the same excitation energy. If the difference between p-n and p-p interactions is neglected, the V_0 extracted with the one-component model from the (p,n) data is expected to be smaller than that from the (p,p') scattering by a factor of $\sqrt{2}$. Taking into account that the effective p-n interaction V_{pn} is about three times as strong as the effective p-p interaction V_{pp} in the energy region of interest [41] introduces another factor of $(V_{pp}+V_{pn})/2V_{pn} = 4/(2\times 3) \approx 0.7$, so we expect $V_0^{pp} \approx V_0^{pn}$. However, the differences in the V_0 values between (p,p') and (p,n) reactions for ^{98}Mo and ^{106}Pd indicate $V_0^{pp} \approx 2V_0^{pn}$. It is possible that this difference is attributable to collective effects extending into the continuum region. It should be emphasized, however, that a two-component MSD theory is necessary to give a consistent description of (p,p') and (p,n) reactions with respect to the strength V_0 of the effective interaction, as pointed out in Refs. [16,37].

C. Gradual absorption of reaction flux in P to Q transitions

We present comparison of the experimental angle-integrated (p,p') and (p,n) spectra for ^{98}Mo at 25.6 MeV with the FKK-GNASH calculation in Fig. 16. The calculation gives some underestimation in the (p,p') and (p,n) spectra lying between the ranges dominated by the evaporation and direct processes, as mentioned in Sec. IV B and IV C. The underestimation is probably due to the MSC component because the relative MSC contribution is found to become large in this energy range and it turned out that our MSD calculation reproduces the experimental MSD component quite well using the subtrac-

tion method, as shown in Figs. 4 and 5. The disagreement is expected to be improved if the MSC spectrum has a softer component, or nucleon emission from more complex MSC stages increases. We made a calculation increasing the maximum stage number of the MSC process up to $N = 5$, but failed to reduce the disagreement, since the MSC emission from stages more than $N = 2$ calculated with Eq. (2) is negligibly small.

In the FKK-GNASH code, there is an assumption that all the reaction flux entering the Q chain from P substages with more complex p-h states than $2p$-$1h$ doorway states decays eventually from the equilibrium stage. Thus the MSC emission of $P \rightarrow Q$ flux from the intermediate N stages is not treated explicitly in our calculations. If one considers the MSC emission after $P \rightarrow Q$ transitions from more complex stages, one can expect the MSC emission spectrum to contain softer components. Such possibilities of the linking between MSD and MSC processes have been pointed out by some authors [11,12,14]. Marcinkowski *et al.* [12] have proposed an idea called "the gradual absorption of reaction flux" in the entrance channels and derived a modified FKK model of the MSC calculation on the basis of phase space arguments. According to their modification, the differential MSC cross section is given

$$\frac{d\sigma}{dE} = \pi\lambda^2 \sum_J (2J+1) \sum_M R_M T_J \sum_{N=M}^{r} \sum_{\nu l} \frac{\langle \Gamma_{nJ}^{\uparrow \nu l}(U) \rangle}{\langle \Gamma_{nJ} \rangle} \times \left(\prod_{m=M}^{N-1} \frac{\langle \Gamma_{mJ}^{\downarrow} \rangle}{\langle \Gamma_{mJ} \rangle} \right), \tag{8}$$

where $R_M T_J$ is the transmission coefficient forming bound states at stage M of spin J multiplied by a reduction factor R_M. The R_M factor can be estimated using the following expression given by the ratio of the restricted to unrestricted Williams formulas of the partial state density, $\omega^B_{np,mh}(E)$ and $\omega_{np,mh}(E)$:

$$R_M = (R - R_1 - R_2 - \cdots - R_{M-1}) \frac{\omega^B_{(M+1)p,Mh}(E)}{\omega_{(M+1)p,Mh}(E)}, \tag{9}$$

where R stands for the reduction of incoming flux by MSD processes and is defined by $(\sigma_R - \sigma_{\rm MSD})/\sigma_R$ with the total reaction cross section σ_R and the total MSD cross section $\sigma_{\rm MSD}$ including the collective excitation. Note that Eq. (8) reduces to the same MSC expression as given in Eq. (4) if one puts $R = 1$ and $M = 1$ in Eqs. (8) and (9).

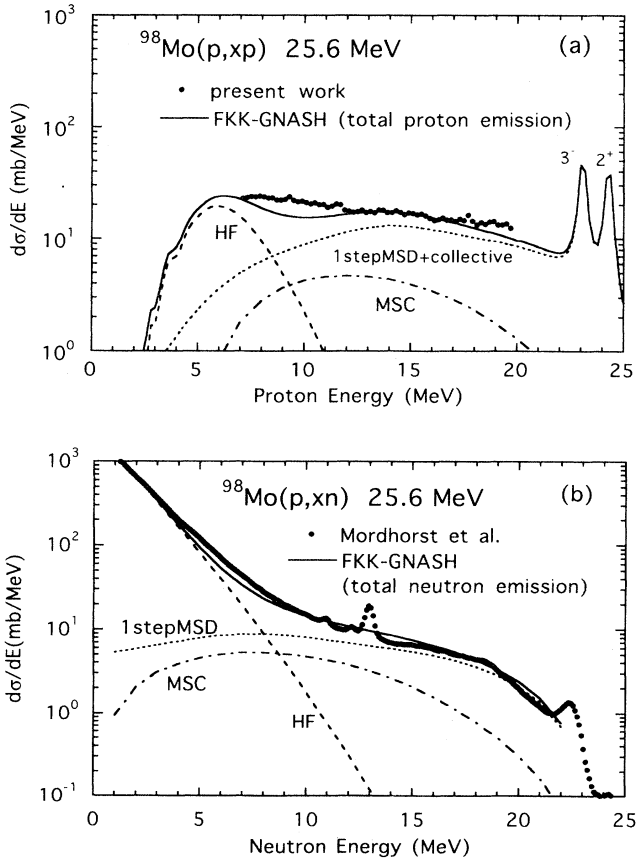

FIG. 16. Comparison of the angle-integrated nucleon emission spectra of the p+^{98}Mo reaction at 25.6 MeV with the FKK-GNASH calculations: (a) proton emission spectra and (b) neutron emission spectra. The experimental data of the (p, xn) spectrum are taken from Ref. [6].

We have implemented an MSC calculation based on Eq. (8) using a modified version of the FKK-GNASH code for several of the reactions listed in Table I. The results of (p,p') and (p,n) on ^{98}Mo at 25.6 MeV are shown in Fig. 17. The maximum number of stages which we considered was $M = 5$. The underprediction seen for both proton and neutron emission in Fig. 16 is obviously improved by the MSC calculation taking into account the gradual absorption effect given by Eq. (8), although some overestimation is seen in the emission energy range between 10 and 15 MeV of the (p,n) spectrum. The use of Eq. (8) was found to lead to the enhancement of MSC emission of nucleons with low energies. A similar improvement was obtained for the ^{106}Pd (p,p') and (p,n) at 26 MeV. These results confirm that the effect of the MSD-MSC crossover in preequilibrium processes is important.

Next, we have applied the modified FKK-GNASH code to other (p,p') reactions at lower incident energies below 18 MeV in order to see the effect of the gradual absorption. The results for 12 and 18 MeV (p,p') on ^{98}Mo are shown in Fig. 18. In contrast with the case of 25.6 MeV in Fig. 17, the modified FKK-GNASH calculation gives no satisfactory description of the energy spectra, especially in the low outgoing energy region. Here we have to recall that the MSD component was determined unambiguously by the subtraction method that gave good agreement between the experimental and calculated spectra. Therefore the disagreement seems be due to MSC and/or HF equilibrium calculations. As shown in Fig. 18, it was found that the MSC emission is not enhanced as much as the case of 25.6 MeV (p, xp) even if the gradual absorption is taken into account. In addition, the GNASH

calculation with the same input parameters as used in the 25.6 MeV (p, xp) reaction provides a very small equilibrium component as the incident energy decreases. As a result, a large modification to the level density parameter of ^{98}Mo depending on the incident energy is required to enhance the HF component of the (p, p') scattering. Also, the disagreement was not improved by using different OMP parameter sets. If one uses the present FKK-GNASH code, therefore, it seems impossible to find a consistent input parameter set to provide a good description of the low emission energy portion of the ^{98}Mo(p, p') spectra for low incident energies below 18 MeV.

One possibility to resolve the underprediction is to incorporate isospin conservation in the MSC and equilibrium calculations. Some previous work based on the exciton model [8,9,42,43] and the statistical multistep reaction model by Kalka [44] have so far shown that isospin conservation is essential in preequilibrium proton emission in proton-induced reactions at low incident energies. Two possible isospin states, with $T_< = T_0 - \frac{1}{2}$ and $T_> = T_0 + \frac{1}{2}$, can be excited in the composite nucleus formed by the proton bombardment, where T_0 is the isospin of the target nucleus. Neutron decay from the $T_>$ states is remarkably suppressed owing to the isospin selection rule, if the excitation energy of the compound nucleus is not high enough compared with the threshold of neutron decay and the mixing between $T_>$ and $T_<$ states is negligible. Thus the isospin conservation can become a major factor to enhance proton emission in MSC and equilibrium processes at low incident energies. If no mixing between $T_>$ and $T_<$ states is assumed, proton emission from more complex preequilibrium stages in the $T_>$ states dominates and a softer energy spectrum is expected, as shown in Ref. [9]. Such proton emission decreases rapidly with increasing incident energy, or excitation energy of the compound nucleus, because the number of states of the residual nucleus accessible by neutron emission from $T_>$ states becomes so large. These considerations would lead to a consistent explanation of our successful FKK-GNASH description for 25.6 MeV and our failure for the lower energies. To justify this interpretation, we will need to extend our MSC and HF calculations so as to take into account isospin as a quantum number. The extension is now in progress. The details of the isospin conservation in MSC and equilibrium processes will be discussed in a forthcoming paper.

VI. SUMMARY AND CONCLUSIONS

We have measured double-differential proton emission cross sections for proton-induced reactions on ^{98}Mo and

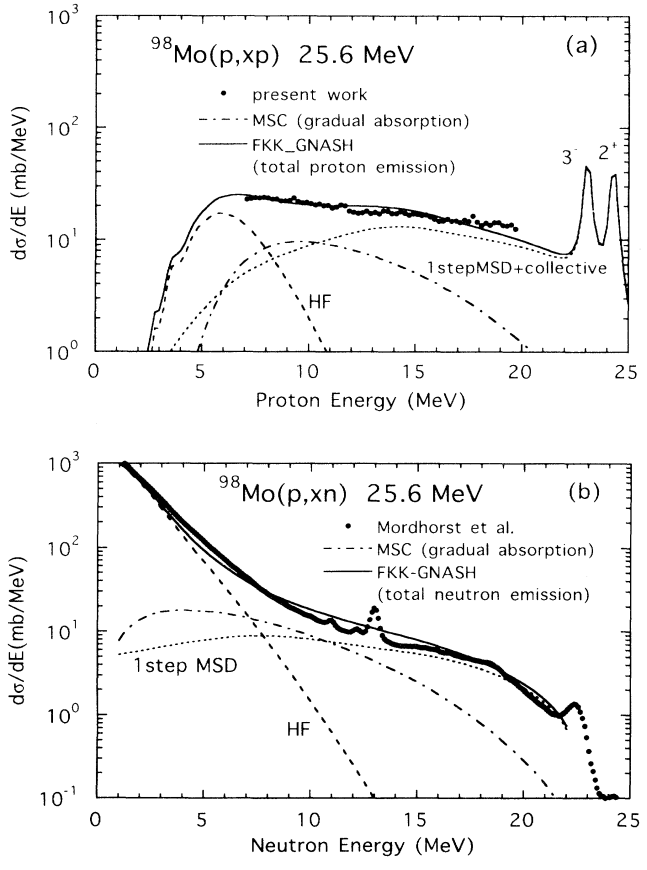

FIG. 17. Same as Fig. 16, but the MSC component is calculated with the FKK-GNASH code modified so as to take into account the gradual absorption effect.

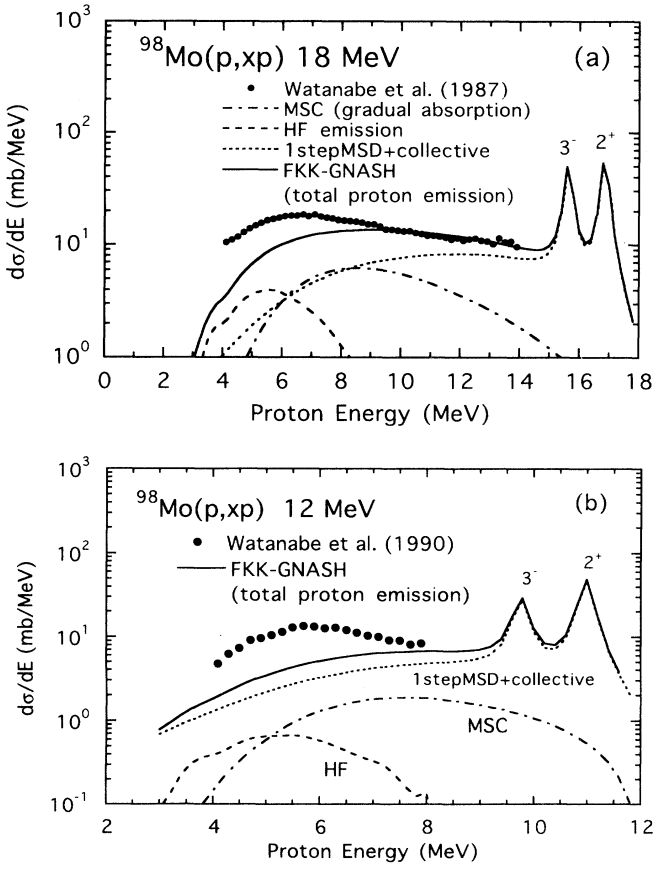

FIG. 18. Comparison of the angle-integrated nucleon emission spectra of the p+^{98}Mo reaction at (a) 12 MeV and (b) 18 MeV with the modified FKK-GNASH code. The experimental data are taken from Refs. [8,9].

^{106}Pd at energies around 26 MeV for which neutron emission data are also available, in order to investigate preequilibrium nucleon emission in the low incident energy region below 30 MeV.

The data on (p,p') and (p,n) reactions for both target nuclei were analyzed using the FKK-GNASH code [10] based on the FKK theory, together with (p,p') for the same target nuclei at energies from 12 to 18 MeV and ^{93}Nb (p,p') and (n,n') at energies from 14 to 26 MeV. The experimental nucleon emission spectra were reproduced quite satisfactorily with the calculation taking into account preequilibrium MSD and MSC emission, direct collective excitation to low-lying discrete levels, and Hauser-Feshbach equilibrium emission, although some underestimation is seen in the low emission region of the (p,p') spectra for incident energies lower than 18 MeV.

In our analyses, we have applied the subtraction method [13] successfully to extract the effective interaction strength V_0 and proved that the method is quite useful for analysis of the MSD component even in the case where large MSC and equilibrium components exist in the particle emission spectra. We have investigated the systematic behavior of the extracted V_0 values. First, the V_0 values for (p,p') were found to vary with an energy dependence of const$/\sqrt{E_{\rm inc}}$, where $E_{\rm inc}$ is the incident energy. Next, the analysis of (p,p') and (n,n') at the same incident energies indicates that the V_0 values of (n,n') are smaller than those of (p,p') and have a weaker energy dependence than those of (p,p'). If the extracted V_0 values of (n,n') and (p,p') are plotted against the local energy of the incident nucleon at the nuclear surface, including the effect of the Coulomb potentials and the difference in the isospin terms of optical potentials, they show a rather smooth variation with the local energy. This seems to be a possible interpretation of the incident energy dependence of the effective N-N interaction used in the FKK analysis in the low incident energy region. Third, the analysis of (p,p') and (p,n) for the same target nucleus and incident energy showed that the extracted strength V_0s differ by a factor of about 2. The reason for the difference is possibly the presence of collective excitations extending into the continuum region in (p,p') scattering. Therefore the inclusion of collective excitations and also a two-component model which can take account of the neutron and proton distinguishability will be necessary to make a simultaneous analysis of neutron and proton emission in nucleon-induced reactions.

Furthermore, the sensitivity of the MSD spectrum to several input parameters and corrections was examined in this work. It was found that the optical potentials sensitively affect the magnitude of the MSD cross section, but not the shape of the spectra. This means that the extracted V_0 values depend strongly upon the choice of the optical potentials. Next, the effect of pairing corrections on the calculated (p,p') spectra was investigated from the viewpoint of the odd-even mass effect on the preequilibrium spectra. On the basis of several observations that there is no appreciable odd-even effect in the preequilibrium spectra, we have proposed the option of no pairing correction to all MSD and MSC calculations. As a result, the agreement between the calculation and the experimental (p,p') for even-even target ^{98}Mo was remarkably improved in the continuum region just above the excitation energy region where there appears a characteristic peak structure corresponding to collective excitation. The effect of the nonlocality of distorting potentials was also investigated and the correction with the Perey factor was found to result in larger values of V_0, compared with the analysis without the correction.

In our comparison between the experimental (p,p') and (p,n) spectra at 26 MeV and the FKK-GNASH calculation, some underestimation was seen in the intermediate emission energy region lying between evaporation and one-step MSD emission. Inclusion of the gradual absorption effect in $P \rightarrow Q$ transitions in the MSC calculation led to an enhancement of the MSC emission from more complex stages and the underestimation was reduced. In the calculation, the MSC calculation part in the FKK-GNASH code was modified in terms of the formulation based on the phase space model [12]. This confirms that the MSD-MSC crossover transitions are important in preequilibrium nucleon emission.

The disagreement at low outgoing energies seen in (p,p') spectra for incident energies lower than 18 MeV was not reduced even if the gradual absorption effect was taken into account in the MSC calculation. Neglect of isospin conservation in our analysis seems to be one of the major reasons for the discrepancy, because proton emission from more complex MSC stages and/or the equilibrium stage is enhanced when neutron emission is remarkably suppressed in particle decay from $T_>$ states of the composite nucleus owing to the isospin selection rule. To demonstrate the importance of isospin conservation in (p,p') reaction at low energies, it will be necessary to include the isospin as well as the spin and angular momentum in the FKK-GNASH calculation.

In the future, we intend to make FKK-GNASH analyses with a standard parameter set for a variety of data of nucleon-induced reactions in order to establish the systematics on the only adjustable parameter V_0. Such analyses will be useful to apply quantum-mechanical model codes, such as the FKK-GNASH code, to nuclear data evaluation involving proton as well as neutron data.

ACKNOWLEDGMENTS

The authors thank the staff of the accelerator division of the JAERI for their kind help during the experiment. One (Y.W.) of the authors wishes to express his thanks to the Grant-in-Aid from the British Council during his stay in Oxford University and the hospitality of the Nuclear Physics Laboratory, Oxford University. Y.W., M.B.C., and P.E.H. thank Dr. W. A. Richter, Dr. M. Avrigeanu, P. Demetriou, and Dr. P. G. Young for valuable discussions on FKK analyses. This work was supported in part by the Grant-in-Aid of the Ministry of Education, Science and Culture in Japan. Also, this work was carried out partly under the auspices of the U.S. Department of Energy by the LLNL under Contract No. W-7405-ENG-48.

[1] H. Feshbach, A. Kerman, and S. Koonin, Ann. Phys. (N.Y.) **125**, 429 (1980).
[2] E. Gadioli and P. E. Hodgson, *Pre-Equilibrium Nuclear Reactions* (Oxford University Press, Oxford, 1992).
[3] R. Bonetti, M. B. Chadwick, P. E. Hodgson, B. V. Carlson, and M. S. Hussein, Phys. Rep. **202**, 171 (1991); R. Bonetti, A. J. Koning, J. M. Akkermans, and P. E. Hodgson, *ibid.* **247**, 1 (1994).
[4] W. Scobel, M. Blann, T. T. Komoto, M. Trabandt, S. M. Grimes, L. F. Hansen, C. Wong, and B. A. Pohl, Phys. Rev. C **30**, 1480 (1984).
[5] Y. Holler, A. Kaminsky, R. Langkau, W. Scobel, M. Trabandt, and R. Bonetti, Nucl. Phys. **A442**, 79 (1985).
[6] E. Mordhorst, M. Trabandt, A. Kaminsky, H. Krause, and W. Scobel, Phys. Rev. C **34**, 103 (1986).
[7] S. Hölbling, R. Caplar, S. Stamer, R. Langkau, and W. Scobel, Z. Phys. A **338**, 11 (1991).
[8] Y. Watanabe, I. Kumabe, M. Hyakutake, N. Koori, K. Ogawa, K. Orito, K. Akagi, and N. Oda, Phys. Rev. C **36**, 1325 (1987).
[9] Y. Watanabe, K. Kodaka, Y. Kubo, N. Koori, M. Eriguchi, M. Hanada, and I. Kumabe, Z. Phys. A **336**, 63 (1990).
[10] M. B. Chadwick and P. G. Young, Phys. Rev. C **47**, 2255 (1993).
[11] A. Marcinkowski, J. Rapaport, R. Finlay, X. Aslanoglou, and D. Kielan, Nucl. Phys. **A530**, 75 (1991).
[12] A. Marcinkowski, J. Rapaport, R. Finlay, C. Brient, M. Herman, and M. B. Chadwick, Nucl. Phys. **A561**, 387 (1993).
[13] P. Demetriou, P. Kanjanarat, and P. E. Hodgson, J. Phys. G **19**, L193 (1993); **20**, 1779 (1994).
[14] G. Arbanas, A. K. Kerman, M. B. Chadwick, and F. S. Dietrich, Lawrence Livermore National Laboratory Report No. UCRL-JC-117171, 1994 [Phys. Rev. C (to be published)].
[15] A. Aoto, Y. Watanabe, H. Hane, H. Kashimoto, Y. Koyama, H. Sakaki, Y. Yamanouti, M. Sugimoto, S. Chiba, and N. Koori, Japan Atomic Energy Research Institute Report No. JAERI-M 92-027, 1992, p. 330.
[16] M. B. Chadwick, P. G. Young, D. C. George, and Y. Watanabe, Phys. Rev. C **50**, 996 (1994).
[17] F. C. Williams, Nucl. Phys. **A166**, 231 (1971); E. Betak and J. Dobes, Z. Phys. A **279**, 319 (1976); P. Oblozinsky, Nucl. Phys. **A453**, 127 (1986).
[18] A. Takahashi, M. Gotoh, Y. Sasaki, and H. Sugimoto, Osaka University, OKTAVIAN Report No. A-92-01, 1992.
[19] S. Matsuyama, T. Ito, M. Baba, T. Ohkubo, H. Ide, F. Huang, and N. Hirakawa, Tohoku University, Fast Neutron Laboratory, Report No. NETU-58, 1992, p.6; M. Baba, S. Matsuyama, T. Ito, T. Ohkubo, and H. Hirakawa, J. Nucl. Sci. Technol. **31**, 757 (1994).
[20] A. Marcinkowski, R. W. Finlay, G. Randers-Pehrson, C. E. Brient, R. Kurup, S. Mellema, A. Meigooni, and R. Tailor, Nucl. Sci. Eng. **83**, 13 (1983).
[21] R. L. Walter and P. P. Guss, in Proceedings of the International Conference on Nuclear Data for Basic and Applied Science, Santa Fe, 1985, edited by P. G. Young (Gordon and Breach, New York, 1986), p. 1079.
[22] H. Gruppelaar, *IAEA Advisory Group Meeting on Basic and Applied Problems on Nuclear Level Densities*, edited by M.R. Bhat (Brookhaven National Laboratory, Upton, NY, 1983), p. 143.
[23] F. G. Perey and B. Buck, Nucl. Phys. **32**, 353 (1962).
[24] P. D. Kunz, computer code DWUCK4, University of Colorado (unpublished).
[25] S. Rama, C. H. Malarkey, W. T. Milner, C. W. Nestor, Jr., and P. H. Stelson, At. Data Nucl. Data Tables **36**, 1 (1987).
[26] R. H. Spear, At. Data Nucl. Data Tables **42**, 55 (1989).
[27] P. G. Young, E. D. Arthur, and M. B. Chadwick, Los Alamos National Laboratory Report No. LA-123443-MS, 1992.
[28] A. Gilbert and A. G. W. Cameron, Can. J. Phys. **43**, 1446 (1965).
[29] D. Wilmore and P. E. Hodgson, Nucl. Phys. **55**, 673 (1964).
[30] F. D. Becchetti, Jr., and G. W. Greenlees, Phys. Rev. **182**, 1190 (1964).
[31] W. A. Richter, A. A. Cowley, R. Lindsay, J. J. Lawrie, S. V. Förtsch, J. V. Pilcher, R. Bonetti, and P. E. Hodgson, Phys. Rev. C **46**, 1030 (1992).
[32] F. G. Perey, Phys. Rev. **131**, 745 (1963).
[33] J. J. H. Menet, E. E. Gross, J. J. Malanify, and A. Zucker, Phys. Rev. C **4**, 1114 (1971).
[34] J. Rapaport, V. Kulkarni, and R. W. Finlay, Nucl. Phys. **35**, 676 (1962).
[35] W. Dilg, W. Schantl, H. Vonach, and M. Uhl, Nucl. Phys. **A217**, 269 (1973).
[36] R. Bonetti and C. Chiesa, computer code MSD, University of Milano (unpublished).
[37] Y. Watanabe, M. Avrigeanu, and W. A. Richter, Oxford University Report No. OUNP-93-30, 1993.
[38] Y. Watanabe and M. Kawai, Nucl. Phys. **A560**, 43 (1993).
[39] A. Koning, in *Proceedings of the Symposium on Nuclear Data Evaluation Methodology*, Brookhaven National Laboratory, Upton, New York, 1992, edited by C. Dunford (World Scientific, Singapore, 1993), p. 434.
[40] Y. L. Luo and M. Kawai, Phys. Rev. C **43**, 2367 (1991).
[41] S. M. Austin, in *The (p,n) Reaction and the Nucleon-Nucleon Force*, edited by C. D. Goodman *et al.* (Plenum, New York, 1980), p. 203.
[42] C. Kalbach-Cline, J. R. Huizenga, and H. K. Vonach, Nucl. Phys. **A222**, 405 (1974).
[43] C. Kalbach, S. M. Grimes, and C. Wong, Z. Phys. A **275**, 175 (1975).
[44] H. Kalka, Z. Phys. A **341**, 289 (1992).